



MOLECULAR MODELING OF THE INTERACTION OF TRYPANOCIDE GUANYL HYDRAZONES WITH B-DNA

Osvaldo A. Santos-Filho, J. Daniel Figueroa-Villar*

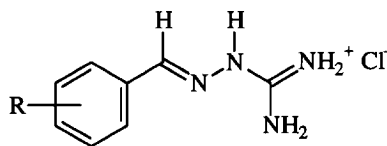
*Departamento de Química, Instituto Militar de Engenharia, Praça General Tibúrcio 80,
22290-270, Rio de Janeiro-RJ, Brazil*

Martha T. Araujo

*Departamento de Físico-Química, Universidade Federal Fluminense, Outeiro de São João Batista, s/n, 24020-
150, Niterói-RJ, Brazil*

Abstract. Molecular modeling of the interaction of trypanocide aromatic guanyl hydrazones with B-DNA showed that the preferential sites for interaction are the DNA minor groove AT rich regions, with hydrogen bonding between the guanidine moiety of the drugs and the thymine O2, and the adenine N3. There is a correlation between the total interaction energy and ID₅₀. © 1997 Elsevier Science Ltd.

Chagas' disease is a serious Latin American illness, caused by the protozoa *Trypanosoma cruzi*, and is responsible for much death and suffering in South America. The current chemicals used to treat this illness are nifurtimox and benznidazol, both of which are not efficient when used to treat the chronic stage of the disease and are toxic to the patients.^{1,2} We have recently reported a new family of compounds that are active against the trypomastigote forms of *T. cruzi*, the aromatic guanyl hydrazones (**1**).³



The mechanism of action of these compounds, some of which are up to 25 times more active than the current drugs,³ may occur in three different ways: (a) interaction with the trypanosome membranes, which are negatively charged; (b) interaction with some specific enzyme of the parasite, and (c) interaction with its DNA. In this work we investigate this last possibility, which is supported by previous experimental studies on the interaction between other cationic drugs and DNA.⁴⁻⁶

In order to accomplish a preliminary molecular modeling of the interactions of the guanyl hydrazones with B-DNA, we selected, according to their biological activity, the 7 representative compounds shown in Table 1. NOE experiments⁷ done on these molecules indicated that they were obtained in the *E* configuration.⁸

We first carried out a complete conformational analysis of each guanyl hydrazone in the *E* configuration using the AM1 semiempirical method⁹ and the CVFF force field.¹⁰ This last one from the Discover 2.95[®] molecular mechanics package.¹¹ The B-DNA dodecamer d(CGCGAATTCGCG) was minimized using the AMBER force field,¹²⁻¹⁴ and then used for the simulations of its interaction with the most stable conformer of each drug using the docking methodology,¹⁵⁻¹⁷ also from the Discover 2.95[®] package, in a IRIS Indigo Silicon Graphics[®] workstation. The best relative position of each drug in relation to the B-DNA double helix was found by monitoring the intermolecular energy while manually changing the relative position of the drug and simultaneously searching for the complementarity between the Connolly surfaces of both molecules.¹⁸ It was found that the B-DNA double helix preferential site for interaction with the guanyl hydrazones is the minor groove. The next step was the minimization of the drug inside the minor groove of the DNA using the optimizers¹⁹ steepest descent, conjugate gradient and quasi-Newton-Raphson until an energy gradient of 0.01 kcal mol⁻¹ Å⁻¹ was obtained. This process is necessary to allow the optimization of the manually model-built drug orientation to seek maximal interaction with the DNA.²⁰ Finally, the whole DNA-guanyl hydrazone complex was minimized, without any constraints, using the CVFF force field. In this last stage, the optimizers steepest descent and conjugate gradient were used until an energy gradient of 1.00 kcal mol⁻¹ Å⁻¹ was obtained. This procedure avoids the occurrence of fortuitously overlapping atoms in the model. All the simulations were carried out using a cut off distance of 5 Å.

It must be pointed out that, in the docking methodology, the total intermolecular energy between two molecules is computed by non bonded terms of a force field equation.^{10,21} This equation for the CVFF force field is shown below:¹¹

$$E_{inter} = \sum \sum (A_{ij} / r_{ij}^{12} - B_{ij} / r_{ij}^6 + q_i q_j / \epsilon r_{ij}),$$

where the two first terms are the Lennard-Jones (6-12) potential and the last one is the Coulomb potential. As we carried out our the simulation in vacuum we employed a distance-dependent dielectric, $\epsilon_{r_{ij}}$, even 1. The results are summarized in Table 1.

It can be observed that the most active compounds have stronger interactions with the B-DNA. To investigate these results in a more quantitative way, we carried out a linear regression analysis using the mean squares method from the SAS package.²² The plots of the total intermolecular energy between the guanyl hydrazones and the B-DNA, as a function of log ID₅₀, are shown in Figures 1 and 2.

Table 1. Total intermolecular energy between the guanyl hydrazones and the B-DNA dodecamer d(CGCGAATTCGCG) and the ID₅₀ of each guanyl hydrazone.

Compound	R	Total intermolecular energy (kcal)	ID ₅₀ (μM)
A	2,3-dimethoxy	-281.90	22.5
B	2-bromo-4,5-methylenedioxy	-268.70	23.7
C	4-chloro	-283.91	27.4
D	H	-278.58	204.9
E	4,5-methylenedioxy	-276.18	273.9
F	2-hydroxy-3-nitro	-270.66	876.7
G	3-methoxy-4-hydroxy	-266.38	4800

When all the data set is used the correlation between the total interaction energy and ID₅₀ is not good ($R^2 = 0.41$) because compound **B** behaves very differently from all other compounds (Figure 1a). Although we have not found a clear explanation for this fact, we believe that this behavior may be due to a synergetic effect between the fused methylenedioxy group and the bromo group in the *ortho* position of the aromatic ring in **B**. If compound **B** is taken out of the analysis a correlation index (R^2) of 0.95 is found (Figure 1b). Although the relevance of this correlation may not be definitely confirmed with the available data, its meaningfulness is being tested with other guanyl hydrazones. The results of this work are being used to choose the next synthetic targets in our search for better anti-trypanosome agents.

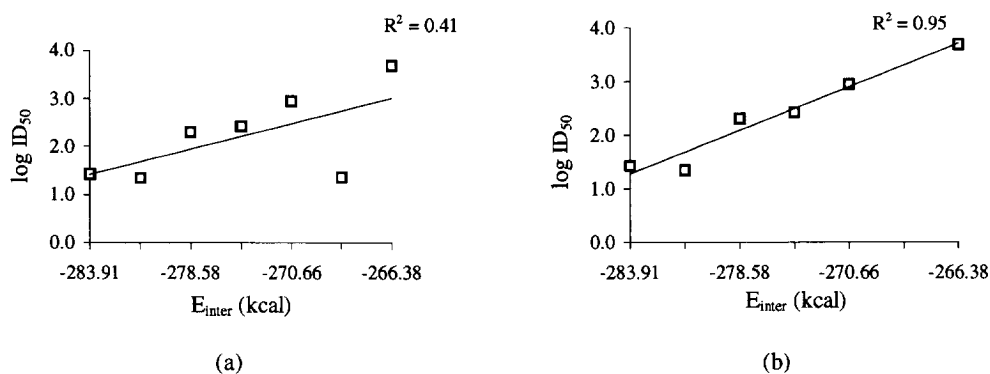


Figure 1. Correlation between the intermolecular energy (E_{inter}) and ID₅₀: (a) of all the drugs ($R^2 = 0.41$) and (b) of all the drugs excluding compound **B** ($R^2 = 0.95$).

A clear lateral view of the complex of the guanyl hydrazone of benzaldehyde (ID₅₀ 204.9 μ M) and the minor groove of B-DNA dodecamer d(CGCGAATTCGCG) is presented in Figure 3. It can be observed that there is a very good shape complementarity between both Connolly surfaces and that the interaction involves the guanidine moiety of the drug while its aromatic ring remains in the outer side of the groove. In Figure 3 it can also be observed that the aromatic ring is not coplanar with the guanyl hydrazone moiety in the complex, in agreement with our previous observation that a good molecular characteristic for activity is to have *ortho*-substitution.⁴



Figure 3. Interaction between compound **D** and the B-DNA dodecamer d(CGCGAATTCGCG).

In fact, all the complexed active drugs presented an angle between the aromatic ring and the hydrazone planes greater than 43°, as shown in Table 2. This angle changes when a comparison is made between the most stable conformer calculated with AM1 and the minimized conformation in the complex. Moreover, there seems to be no correlation between this angle change and ID₅₀, nor between the corresponding energy change and ID₅₀.

The two less active drugs of this sample are those that present hydroxyl groups at the aromatic ring, but no evidence of how this molecular singularity affects the formation of the complexes was found. It seems that the guanyl hydrazone group has the optimal length for this kind of interaction (6.0 to 6.1 Å). In all the cases studied the B-DNA preferential site for interaction with the guanyl hydrazones is the AT rich region in the minor groove, and it seems that this interaction occurs through hydrogen bonding between the guanidine moiety of the drugs and the thymine O2 (as shown in Figure 3) and/or the adenine N3 of the B-DNA. This kind of interaction with DNA have been found for other cationic drugs.^{5,6} One explanation for this preferential docking with AT rich regions was given by Pullmann *et al.*,^{23,24} who made theoretical studies of the interaction between cationic

compounds and B-DNA. Their study showed the predominant role played by the distribution of the electrostatic potential in the minor grooves of nucleic acids, the most negative values being found in the minor groove of AT rich sequences.

Table 2. Dihedral angle ϕ between the aromatic ring plane and the guanyl hydrazone plane.

Compound	ϕ in the free form (degrees)	ϕ in the complex (degrees)	$\Delta\phi$ (degrees)	ΔE (kcal)	ID ₅₀ (μ M)
A	56.64	43.06	13.58	-28.68	22.50
B	85.18	73.29	11.89	-22.81	23.70
C	39.22	79.34	-40.12	-18.94	27.40
D	55.25	46.66	8.59	-17.21	204.9
E	51.08	68.65	-17.57	-22.27	273.9
F	50.57	38.85	11.72	-28.07	876.7
G	57.08	38.10	18.98	-25.83	4800

Our analysis shows that interaction with the minor groove of DNA is a plausible mechanism of action for these compounds. The selectivity of this action against *Trypanosoma cruzi*, when compared to mammal cells, may be due to facilitated permeation through the parasite cell membrane, induced by selective binding of the drugs to the negatively charged exterior of the parasite.

Acknowledgments

We are grateful to the PADCT/CNPq and CAPES for financial support.

References

1. Gutteridge, W. E. *British Med. Bull.* **1985**, *41*, 162.
2. Marr, J. J.; Docampo, R. *Rev. Infec. Diseases* **1986**, *8*, 884.
3. Messeder, J. C.; Tinoco, L. W.; Figueroa-Villar, J. D.; Souza, E. M.; Santa Rita, R.; de Castro, S. L. *Bioorg. Med. Chem. Lett.* **1995**, *5*, 3079.
4. Cory, M. *Med. Chem. Res.* **1992**, *1*, 417.

5. Dabrowiak, J. C.; Stankus, A. A.; Goodisman, J. In *Nucleic Acid Targeted Drug Design*; Propst, C. L.; Perun, T. J., Ed.; Marcel Dekker: New York, 1992; pp 93-149.
6. Kopka, M. L.; Larsen, T. A. In *Nucleic Acid Targeted Drug Design*; Propst, C. L.; Perun, T. J., Ed.; Marcel Dekker: New York, 1992; pp 303-374.
7. Derome, A. E. *Modern NMR Techniques for Chemistry Research*; Pergamon Press: New York, 1987; pp 97-127.
8. Unpublished result.
9. Dewar, M. J. S.; Zoebisch, E. G.; Healy, E. F.; Stewart, J. J. P. *J. Am. Chem. Soc.* **1985**, *107*, 3902.
10. Burkert, U.; Allinger, N. L. *Molecular Mechanics*; American Chemical Society: Washington, DC, 1982.
11. DISCOVER[®], version 2.9.5 & 94.0 - User Guide, Part 1. BIOSYM Technologies, San Diego, 1994.
12. Weiner, P. K.; Kollman, P. A. *J. Comput. Chem.* **1981**, *2*, 287.
13. Weiner, S. J.; Kollman, P. A.; Case, D. A.; Singh, U. C.; Ghio, C.; Alagona, G.; Profeta Jr., S.; Weiner, P. J. *Am. Chem. Soc.* **1984**, *106*, 765.
14. Weiner, S. J.; Kollman, P. A.; Nguyen, D. T.; Case, D. A. *J. Comput. Chem.* **1986**, *7*, 230.
15. Kuntz, I. D.; Blaney, J. M.; Oatley, S. J.; Langridge, R.; Ferrin, T. E. *J. Mol. Biol.* **1982**, *161*, 269.
16. DesJarlais, R. L.; Sheridan, R. P.; Seibel, G. L.; Dixon, J. S.; Kuntz, I. D.; Venkataraghavan, R. *J. Med. Chem.* **1988**, *31*, 722.
17. Pattabiraman, N.; Levitt, M.; Ferrin, T. E.; Langridge, R. *J. Comput. Chem.* **1985**, *6*, 432.
18. Connolly, M. L. *Science* **1983**, *221*, 709.
19. Press, W. H.; Flannery, B. P.; Tenkosky, S. A.; Vetterling, W. T. *Numerical Recipes*; Cambridge University Press: London, 1989.
20. Rao, S. N. In *Nucleic Acid Targeted Drug Design*; Propst, C. L.; Perun, T. J., Ed.; Marcel Dekker: New York, 1992; pp 65-91.
21. Grant, G. H.; Richards, W. G. *Computational Chemistry*; Oxford University Press: New York, 1995.
22. SAS Institute Inc., Cary, NC, U.S.A, 1985.
23. Bonaccorsi, R.; Pullman, A.; Scrocco, E.; Tomasi, J. *Theoret. Chim. Acta (Berl.)* **1972**, *24*, 51.
24. Lavery, R.; Pullman, B. *Int. J. Quantum Chem.* **1981**, *20*, 259.

(Received in USA 11 April 1997; accepted 9 June 1997)